Gravity Probe B Gyroscope charge control using field-emission cathodes

Saps Buchman, Theodore Quinn, G. M. Keiser, and Dale Gill
Gravity Probe B Program, W. W. Hansen Experimental Physics Laboratory, Stanford University, Stanford, California 94305-4805

(Received 13 July 1992; accepted 27 November 1992)

We propose and test a method for controlling the charging of the Gravity Probe B(GP-B) electrostatically suspended gyroscopes using electrons generated by field emission cathodes. The GP-B Gyroscope Experiment is designed to measure for the first time the geodetic and the frame-dragging effects predicted by Einstein's general theory of relativity. The expected accuracy of ~0.3 marcsec/yr (10^{-11} deg/h) will allow for a 0.01% measurement of the geodetic effect and a 1% measurement of the frame-dragging effect. Gyroscope charging is caused by cosmic radiation, by field emission, and by the separation of dissimilar metals. The expected charging rate for the gyroscopes is ~1 nC/yr and consequently above the 50 pC limit dictated by disturbing torque considerations. The present charge control technique is based on ultraviolet photoemission of electrons from both the gyroscope and an auxiliary electrode. Experiments have shown this method to be effective at room temperature in ground testing, and calculations indicate that it is suitable for charge control in orbit. As an alternative we demonstrate the use of Spindt-type field emission cathodes for the control of the positive charges on the gyroscopes, by using a 10 000 tip emitter array produced by SRI International. The device requirements are (a) stable and reliable operation over two years at 2 K and 1.5×10^{-9} Pa, (b) average power dissipation in the device of less than 50 μW, (c) peak emission current of 1–100 pA, (d) dimensions less than 2 mm, (e) magnetization less than 10^{-8} G, (f) electric field at the gyroscope less than 10^4 V/m. The control of negative charges on the gyroscope is achievable by operating in a regime in which the secondary electron emission coefficient is greater than unity.

I. INTRODUCTION

The GP-B Relativity Gyroscope Experiment[1] will measure for the first time the geodetic and the frame-dragging effects predicted by Einstein's general theory of relativity. Schiff[2] calculates the relativistic precession rate of an ideal free-falling gyroscope with respect to the frame of the distant stars to be

$$\Omega=\frac{3GM}{2c^2R^3}(\mathbf{R}\times\mathbf{v})+\frac{GI}{c^2R^3}\left[\frac{3\mathbf{R}}{R^2}\times(\omega_e\times\mathbf{R})-\omega_e\right], \quad (1)$$

where **R** and **v** are the position and the orbital velocity of the gyroscope, and M, I, and ω_e are the mass, the moment of inertia, and the angular velocity of the central rotating sphere. The first term gives the geodetic precession due to the gravitational field of the central body, while the second term represents the frame-dragging precession due to the rotation of the central body.

The experiment will take place in a drag-free satellite in a 650 km high polar orbit. For these conditions, the geodetic precession is calculated to be 6.6 arcsec/yr and the frame dragging precession is 0.042 arcsec/yr (Fig. 1). The measurement is performed by comparing the local reference frame defined by the GP-B gyroscopes (Fig. 2), to the reference frame of the distant stars defined by the line of sight to Rigel. We expect an accuracy of about 0.3 marcsec/yr (10^{-11} deg/h) allowing for a 0.01% measurement of the geodetic effect and a 1% measurement of the frame-dragging effect. A precise measurement of these effects will differentiate between competing gravitational theories, and will contribute to the understanding of astrophysical observations.

The requirement of 10^{-11} deg/h long term stability for the GP-B gyroscopes is significantly more exacting than the 10^{-5} deg/h performance of the best earth-based compensated electrostatically suspended gyroscopes. To achieve this requirement the disturbing torques are reduced by performing a space-based (5×10^{-11} g), low temperature (2 K), ultrahigh vacuum (1.5×10^{-9} Pa) experiment. The GP-B gyroscopes are electrostatically suspended, niobium-coated quartz balls, of 2 cm radius, with a peak-to-valley asphericity of less than 25 nm, and a spin frequency of 170 Hz. In order to eliminate differential contraction effects, the gyroscope housing is also made of quartz with three pairs of orthogonal sputtered thin-film suspension electrodes.

We use the London moment[3] as the basis for the GP-B gyroscope readout. A rotating superconductor produces throughout its volume a uniform magnetic field $\mathbf{B}_L$ aligned with the instantaneous spin axis ω_s of magnitude:

$$\mathbf{B}_L=-\frac{2mc}{e}\omega_s=-1.14\times10^{-7}\,\omega_s\ \text{G}, \quad (2)$$

where m and e are the mass and the charge of the electron. A spherical gyroscope of radius r produces a magnetic dipole $\mathbf{M}_L$ (London moment) given by:

$$\mathbf{M}_L=-\frac{mc}{e}r^3\omega_s=-5.69\times10^{-8}\,r^3\omega_s\ \text{G cm}^3. \quad (3)$$

 0734-211X/93/020407-05$01.00

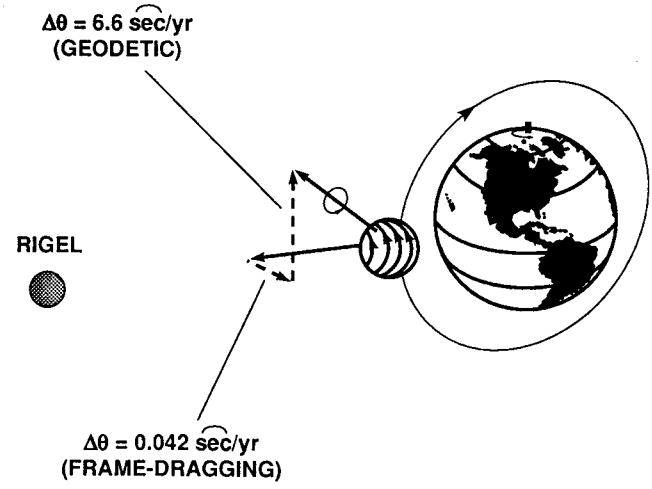

FIG. 1. GP-B geodetic and frame-dragging precessions predicted by general relativity.

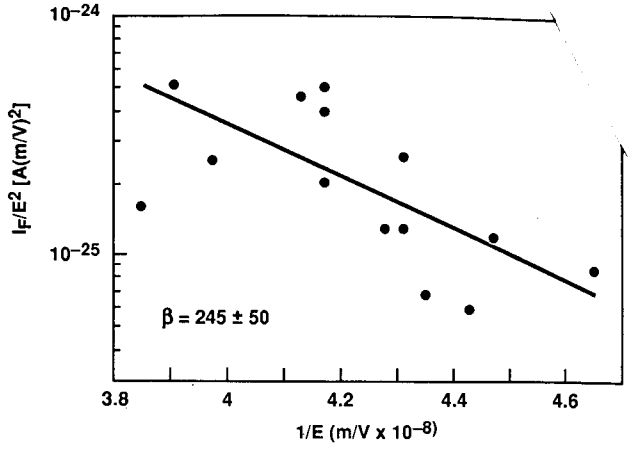

FIG. 3. Fowler–Nordheim plot for a functioning gyroscope.

The London moment is instantaneously aligned with the spin axis, making it uniquely suitable as a gyroscope readout.

This article discusses the problem of charge buildup on the gyroscopes and two methods of controlling this charging. Electrical charges produce electrostatic torques on the gyroscope and instabilities in the suspension system, thus imposing an upper limit requirement of 50 pC for the gyroscope charge. The first method of charge control is based on electron photoemission by 254 nm UV photons piped to the gyroscope through optical fibers.[4] We demonstrate the use of a Spindt-type field emission cathode[5,6] mounted in the gyroscope housing as an alternative charge control method.

II. GYROSCOPE CHARGING MECHANISMS

Enhanced field emission, caused by the large electric fields ($\sim 3\times 10^7$ V/m) required for electrostatic levitation, is the principal mechanism for gyroscope charging during ground testing. Asymmetry in the enhanced field emission between the niobium coating of the gyroscope and the titanium coating of the electrodes results in a predominantly negative charging of the gyroscope. In orbit the levitation fields will be reduced to 10^7 V/m during gas spinup and to 10^4 V/m for regular operation. Figure 3 shows the Fowler–Nordheim[7] plot for a functioning gyroscope (with β about 250) in which the electrostatic suspension field has been varied between the minimum field necessary for levitation and the maximum field for which the feedback system remained stable. For correctly fabricated and conditioned GP-B gyroscopes the field emission current, at both room and liquid helium temperatures, is in the range 1–10 pA; resulting in a charging rate of 7–70 V/h at the nominal suspension field of 3×10^7 V/m.

The continuous charging of the gyroscopes during the GP-B Science Mission[8,9] will be primarily due to protons trapped in the radiation belt and solar flare protons. Using the Bethe–Bloch formula[10] for energy loss of charged particles in materials, we calculate the energy range of the protons which will come to a stop inside the gyroscope to be between 140 and 205 MeV.[8] For the proton flux in a 650 km polar orbit, and assuming one solar flare per year,[9] the total flux of stopped protons will be $\sim 6\times 10^9$ protons/yr. This translates into a positive potential increase rate of 2.5 V/yr for the 500 pF gyroscope (Fig. 4), which is above the limit of 0.1 V required for normal operation. The insert in Fig. 4 shows the details of daily charging due to trapped protons, and reflects the fact that virtually all trapped protons at this altitude are found in the area of the South Atlantic Anomaly (SAA). The GP-B satellite will pass through the SAA during 5 out of every 8 orbits with a crossing time of about 5 min (out of the 90 min orbital period). A detailed calculation[8] shows that charging by secondary electrons can be neglected, as confirmed by extrapolating the charging data for the proof mass of the CASTOR/CACTUS experiment to the GP-B orbit.[11,12]

Charging will also occur due to gyroscope levitation (separation of dissimilar metals) and spinup of the gyroscope with helium (partially ionized gas). The magnitude and the sign of the charging due to these mechanisms are difficult to predict. Laboratory experiments place an upper bound of ± 10 V on the gyroscope charging they produce.

Table I summarizes the charge control requirements during the different stages of the GP-B space experiment. Included are the requirements for charge control current,

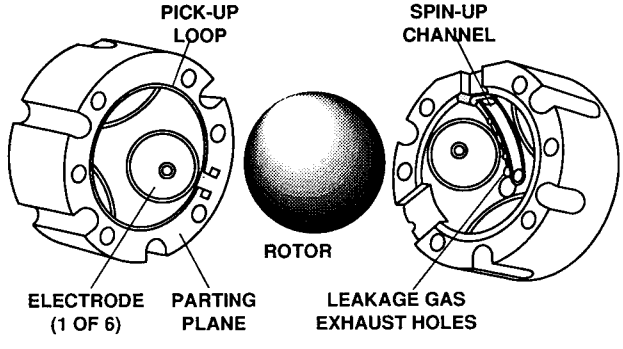

FIG. 2. Exploded view of the GP-B quartz gyroscope assembly.

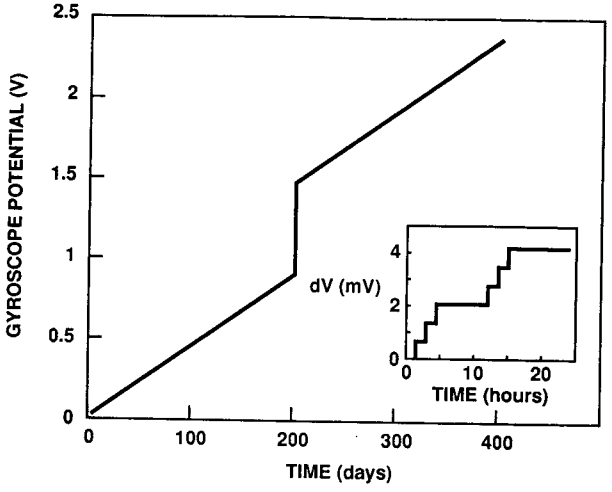

FIG. 4. Calculated gyroscope charging due to trapped and solar flare protons. The orbital period is 1.5 h.

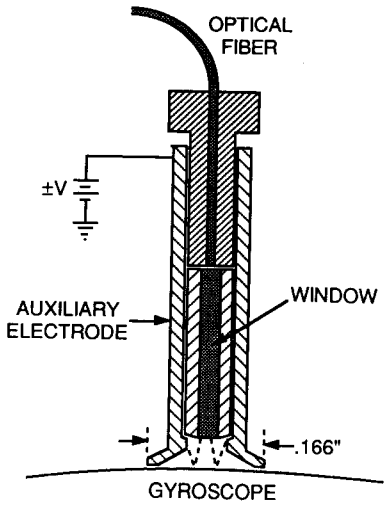

FIG. 5. Schematic representation of the UV charge control assembly with optical fiber.

maximum allowable power dissipated in the gyroscope and in the gyroscope housing, and the duration of each stage. The sign of the current indicates that a source of electrons is required for charge neutralization in regular space operation.

The maximum current required for regular operation is -5×10^{-15} A during solar flares or for continuous charge neutralization during passage through the SAA. Using field emission cathodes charge control would be achieved by millisecond length pulses of 10^{-12}–10^{-10} A. The last row of Table I indicates the current and power requirements averaged over the emission duration. During the experiment initialization the gas pressure is relatively high (10^{-6} Pa), and the increased thermal conductivity allows a higher limit for power dissipation in the gyroscope assembly. The sign of the charging during this period makes it necessary to also provide a method for electron removal from the gyroscope.

III. CHARGE MEASUREMENT AND CONTROL

The force modulation charge measurement method is implemented by applying 180° out of phase excitation voltages $V_C\sin(\omega_C t)$ to two opposite electrodes. The frequency ω_C is set between 10% and 50% of the bandwidth of the suspension servo system, and the excitation voltage V_C at less than 10% of the suspension voltages. The component of the force at frequency ω_C is proportional to the gyroscope potential, and therefore, a measurement of its charge. Note that with the excitation voltage being applied below the bandwidth of the servo system there is no motion of the gyroscope and that to first order the gyroscope potential measurement is independent of the gyroscope position. During space operation a charge measurement excitation voltage of 25 mV will result in an estimated rotor voltage measurement sensitivity of 4 mV for an integration time of 100 s, well below the required 100 mV sensitivity.

TABLE I. Charge control requirements for the GP-B experiment.

Operation period	Duration	Current (A)	Power in gyroscope (W)	Power in housing (W)
Experiment initialization				
Levitation	100 h	$\pm5\times10^{-14}$	10^{-7}	5×10^{-4}
Gas spinup	100 h	$\pm5\times10^{-14}$	10^{-7}	5×10^{-4}
Regular operation				
SAA passage (63% of orbits)	5 min of 90 min orbit	-5×10^{-15}	5×10^{-9}	10^{-4}
Solar flare (1/yr)	100 h	-5×10^{-15}	5×10^{-9}	10^{-4}
Average cosmic radiation	18 000 h	-10^{-16}	10^{-10}	10^{-5}

Charge control of the GP-B gyroscopes requires a controlled source of both positive and negative charges. Possible applicable techniques are radioactive sources, electron field emission, and photoemission. The present charge control technique for GP-B is based on photoemission at the 254 nm UV mercury line. Figure 5 shows the design of the gyroscope with the hardware for photoemission charge control, including a silica fiber for bringing the UV to the cryogenic region and the auxiliary photoemission electrode which mounts in the gyroscope housing. Electrons can be either added to or removed from the gyroscope by controlling the bias on the photoelectrode. The outer layer of the gyroscope coating is niobium and the photoemission electrode is made of titanium. Using 10^{-7}W of 254 nm light, the photoemission current from the gyroscope is 2×10^{-13} A at a bias of 3 V, while the photoemission electrode produces 2×10^{-14} A at a bias of -3 V. The main drawbacks of this method of charge control are the reliability and power consumption (15 W) issues associated with the UV source and fiber optics system and the effect on the gyroscope of the large amount of UV radiation needed for the photoemission of each electron.

An appropriate alternative electron source for GP-B is a Spindt-type field emission cathode. During steady-state op-

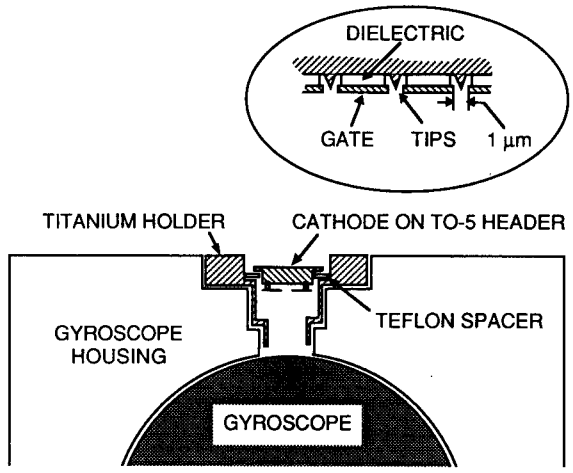

FIG. 6. Schematic representation of the field emission cathode and its holder mounted in the gyroscope housing. Insert shows a schematic cross section of a Spindt-type emission cathode.

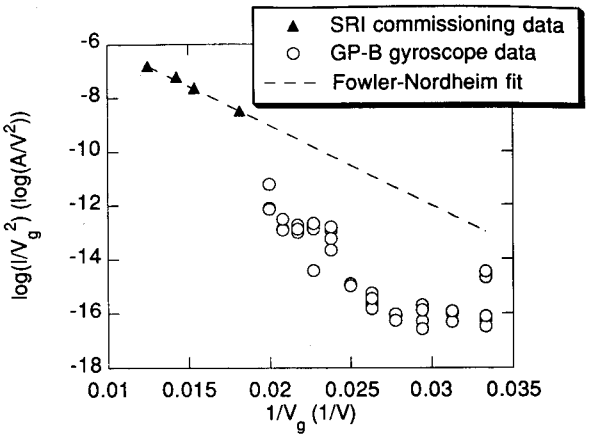

FIG. 8. Fowler–Nordheim plot with SRI commissioning data and GP-B gyroscope data. The dashed line is the Fowler–Nordheim fit to the commissioning data.

eration charging is due to proton capture, and consequently an electron source is adequate for charge control in this regime. We have performed room temperature tests of a field emission cathode installed in a flight type gyroscope under conditions representative of the operational environment. The device we used contains an array of 10 000 tips in a TO-5 header mounting and is supplied by SRI International (cathode 719 A). Figure 6 shows the cathode and its holder installed in the gyroscope assembly. The insert in Fig. 6 represents a schematic cross section of a Spindt-type field emission cathode.

Figure 7 shows the test arrangement used. The holder was connected to the gate and measurements were performed at various gate and collector voltages. In this configuration the gyroscope is the collector. The gyroscope environment prevented us from performing the correct cleaning and conditioning of the cathode, resulting in a lower quality performance than the one achieved by SRI during the commissioning of the device. We did not perform a bakeout of the system or the cathode, and the vacuum level was only 10^{-5} Pa, as compared with the recommended 10^{-7} Pa level. Figure 8 is the Fowler–Nordheim plot for the SRI commissioning data of the cathode and the fit to that data extrapolated to the low gate bias voltages adequate for the gyroscope application. We maintain the emission level at all times below 1 μA, therefore, avoiding damage due to breakdown. The data points for the emission current at 30–50 V gate bias and 20 V collector bias are shown together with the Fowler–Nordheim plot of the commissioning data. The wide scatter in the data is due to the instability in the emission. The emission current is below the Fowler–Nordheim prediction from the commissioning data. Both effects are attributable to the lack of conditioning and bakeout.

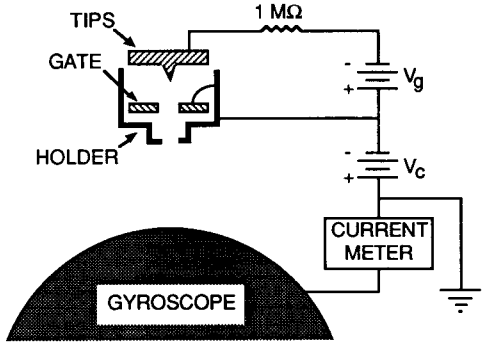

FIG. 7. The experimental arrangement for testing gyroscope charge control using a Spindt-type cathode. V_g and V_c are the gate and collector bias voltages, respectively.

The typical maximum gate current for this type of device is $\sim 10^{-6}$ A resulting in a peak power dissipation in the cathode of 5×10^{-5} W. In addition, we predict a maximum of 5×10^{-5} W dissipation in the holder due to electrons which do not reach the gyroscope. Taking into consideration a duty cycle of less than 1%, the total power dissipation in the cathode and holder is significantly below the allowed maximum for the gyroscope housing. The power dissipated in the gyroscope itself by the 50 eV electrons, at an average current of 10^{-16} A, is only 5×10^{-15} W, and thus, negligible.

Figure 9 shows the dependence of the emission current on the collector voltage at 40 V gate bias. The current delivered to the gyroscope shows little dependence on collector voltage, indicating that the majority of the electrons reach the gyroscope even with no collector bias. This current is significantly higher than the maximum required current of 5×10^{-15} A. The switching time of the cathode is of the order of 1 μs, allowing for short duty cycles in order to reduce the average current to the required level. Grounding the gate and the mounting tube insures a minimum stray electric field at the gyroscopes. This field due to the emitter tips themselves is again well below the requirements.

The GP-B flight requirements will necessitate a repackaging of the cathodes in a smaller envelope and careful use of screened nonmagnetic materials. Reliability tests of long

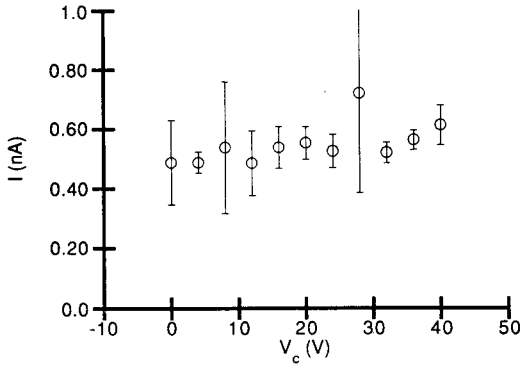

FIG. 9. Current delivered to gyroscope vs collector voltage for a gate voltage of 40 V.

term operation at low temperature will have to be performed, together with mechanical vibration tests. A charge control system using a pulsed Spindt-type field emission cathode and the feedback system from the charge measurement system will be simple to construct and operate. The wiring to the gyroscope and the fixture of the emitter in the gyroscope housing is very simple compared to the equivalent requirements for an UV photoemission system. The power required to operate the emitter is much less than that needed for an UV source.

Negative charging of the gyroscope occurs during ground testing and during the experiment initialization stage in orbit. Neutralization of negative charges is achievable by operating in a regime in which the coefficient for secondary electron emission from the gyroscope is greater than unity. For the oxidized metal surface of the gyroscope this would require electrons with an energy of ~ 500 eV.[13] The disturbing torques produced by a 500 V accelerating voltage are acceptable during ground testing and orbital setup. The field emission cathode charge control system would use a 500 V negative biasing of the entire emitter in order to switch from positive to negative gyroscope charge compensation.

ACKNOWLEDGMENTS

The authors wish to thank C. A. Spindt for its kind help with the field emission cathode, its commissioning, and its operation instructions. Editorial assistance by M. Jarnot is gratefully acknowledged. This work was supported by NASA Contract No. NAS8-36125.

[1]J. P. Turneaure *et al.*, Adv. Space Res. **9**, 29 (1989).
[2]L. I. Schiff, Proc. Natl. Acad. Sci. **46**, 871 (1960).
[3]F. London, *Superfluids* (Dover, New York, 1961), Vol. I.
[4]S. Buchman, M. Keiser, D. Gill, and R. VanPatten (unpublished).
[5]C. A. Spindt, I. Brodie, L. Humphrey, and E. R. Westerberg, J. Appl. Phys. **47**, 5248 (1976).
[6]C. A. Spindt, C. E. Holland, A. Rosengreen, and I. Brodie, IEEE Trans. Electron Devices **ED-38**, 2355 (1991).
[7]R. V. Latham, *High Vacuum Voltage Insulation: The Physical Basis* (Academic, London, 1981).
[8]J. Fiero (private communication, Stanford University, 1990).
[9]W. L. Imhof and J. B. Reagan, J. Geophys. Res. **74**, 5054 (1969).
[10]H. A. Enge, *Introduction to Nuclear Physics* (Addison–Wesley, Reading, MA, 1966).
[11]F. Barlier, (private communication, CERGA, 1990); J. Tiffon, ONERA Technical Note No. 200 (France, 1972).
[12]Y. Boudon, These de doctorat d'Etat, Universite Pierre et Marie Curie, 1984 (unpublished).
[13]B. Chapman, *Glow Discharge Processes* (Wiley, New York, 1980).